



Characterisation of epitaxial TiO₂ thin films grown on MgO(001) using atomic layer deposition

D.R.G. Mitchell*, D.J. Attard, G. Triani

Institute of Materials and Engineering Science, ANSTO, PMB 1, Menai, NSW 2235, Australia

Received 20 June 2005; received in revised form 28 July 2005; accepted 2 August 2005

Available online 21 September 2005

Communicated by M. Kawasaki

Abstract

Thin films of TiO₂ have been deposited onto MgO(001) substrates using atomic layer deposition at 300 °C. Plan and cross-sectional transmission electron microscopy (TEM), X-ray diffraction and atomic force microscopy have been used to understand the nature of the films. X-ray and electron diffraction showed that a polycrystalline, epitaxial anatase film was produced. The *c*-axis of the anatase was parallel to the MgO(001) surface with two orientational variants at right angles to each other in the plane of the film, each aligned with an MgO cube axis. Plan-view and cross-sectional TEM showed that the grain structure of the film reflected this orientation relationship, with the grain morphology comprising two sets of roughly tetragonal grains. Also present was a small fraction of equiaxed, anatase grains which were randomly oriented. Roughness measurement using atomic force microscopy showed that the epitaxial anatase films were quite smooth, in comparison to equivalent non-aligned films grown on silicon. Crown Copyright © 2005 Published by Elsevier B.V. All rights reserved.

PACS: 68.37.Lp; 68.55.–a

Keywords: A1. Transmission electron microscopy; A3. Atomic layer deposition; A3. Epitaxy; B1. MgO substrate; B1. TiO₂

1. Introduction

Atomic layer deposition (ALD) is a well-established technique for depositing thin highly conformal

layers of oxides, nitrides, sulphides etc. [1,2]. The deposition process involves cyclic dosing with reactants which chemisorb onto the substrate surface. Following purging to remove excess reactant, a second reactant is introduced to form the species of interest by reacting with the chemisorbed layer. The surface-limited nature of the reaction [2] results in the growth of highly conformal films, offering a major advantage over line-of-site techniques such as sputtering or evaporation. Film growth takes place

*Corresponding author. Institute of Materials and Engineering Science, ANSTO, New Illawarra Road, Lucas Heights, NSW 2234, Australia. Tel.: +61 2 9717 3456; fax: +61 2 9543 7179.

E-mail address: drm@ansto.gov.au (D.R.G. Mitchell).

at a sub-atomic layer level per deposition cycle. Deposition rates using ALD are often in the range of 50–300 nm/h. Although slow in comparison with many coating techniques, the cyclic nature of the ALD process permits exquisite control over film thickness, with nanometre precision attainable [3,4].

A major effort has been expended in understanding the nature of TiO₂ deposition using ALD [5–8] due to the importance of this material in optical, photochemical, catalytic and sensor applications. The influence of the substrate on TiO₂ film growth has been investigated on substrates including Si (both native oxide covered and hydride terminated) [9], KBr [10] and soda-lime glass [11]. In all instances, at temperatures of around 300 °C, anatase was formed with no preferred orientation. Schuisky et al. [11,12] have investigated titania film growth on α -Al₂O₃(012) and MgO(001) substrates and have demonstrated epitaxial rutile growth on the former and epitaxial anatase growth on the latter. Film–substrate orientation relationships were determined by X-ray and transmission electron microscopy (TEM) methods. The film growth on single-crystal α -Al₂O₃ resulted in a single crystal titania containing twins and/or antiphase domains. However, the epitaxial titania formed on MgO was polycrystalline and occurred in two orientational variants. In this work, we have applied a range of TEM methods along with X-ray diffraction (XRD) and atomic force microscopy (AFM), to better understand the nature of the TiO₂ formed on MgO(001). Of particular interest were the origin of the texturing induced by MgO substrates on ALD TiO₂ films, the grain morphology—bearing in mind the existence of two orientational variants and the influence of the substrate on the growth rate.

2. Experimental procedure

Film deposition was achieved using a Micro-chemistry ALCVD F-120 travelling-wave deposition system, the details of which are given elsewhere [13]. TiO₂ was deposited using TiCl₄ as a source of Ti, water as the nucleophilic source of oxygen and nitrogen as a purge gas. The reactor was operated at a temperature of 300 °C and a

pressure of 10 mbar. The deposition pulsing sequence consisted of a 0.3 s pulse of TiCl₄, followed by a 0.5 s purge of nitrogen, a 0.4 s pulse of water vapour, then a 0.5 s of purge with nitrogen. The film target thickness was 100 nm and 2000 deposition cycles were used.

Specimens for TEM were prepared in plan-view and cross-sectional modes using the methods described elsewhere [9]. The MgO substrate was obtained from MTI Corporation, USA. This exhibited a tendency to break up when thinned below a few microns; presumably from an inherently high level of residual stress. The MgO crystals were in the as-received condition and were not annealed prior to use. Consequently TEM specimens were often much thicker than ideal, as thin regions broke up. TEM specimens were examined using a JEOL 2010F TEM operated at 200 keV. This instrument was fitted with a Gatan imaging filter (GIF) and an X-ray energy dispersive spectroscopy (EDS) system. Film roughness was measured ex situ in air using a Digital Instruments D3000 atomic force microscope with a Nanoscope III controller. The structure and orientation of the titania film on MgO was also examined by a Scintag X1 diffractometer, using a Cu K α 1 and 2 source, with a rotating sample stage. An X-ray pattern was generated using θ – 2θ geometry over the range $2\theta = 20$ – 58° .

3. Results and discussion

Plan-view examination of the film in bright field (Fig. 1a) and dark field (Fig. 1b) modes highlighted the presence of a strong ordering in the film, since the grains were generally rectangular in outline with two main orientations at right angles to each other. Grains were 50–100 nm wide and 100–200 nm in length. This grain size is intermediate to that which we have measured for anatase films deposited under identical conditions on silicon with the native oxide layer present (213 ± 96 nm) and with the oxide layer stripped using HF (17 ± 7 nm) [9]. We also found that very fine grained anatase grew on KBr(001) substrates (22 ± 6 nm) [10].

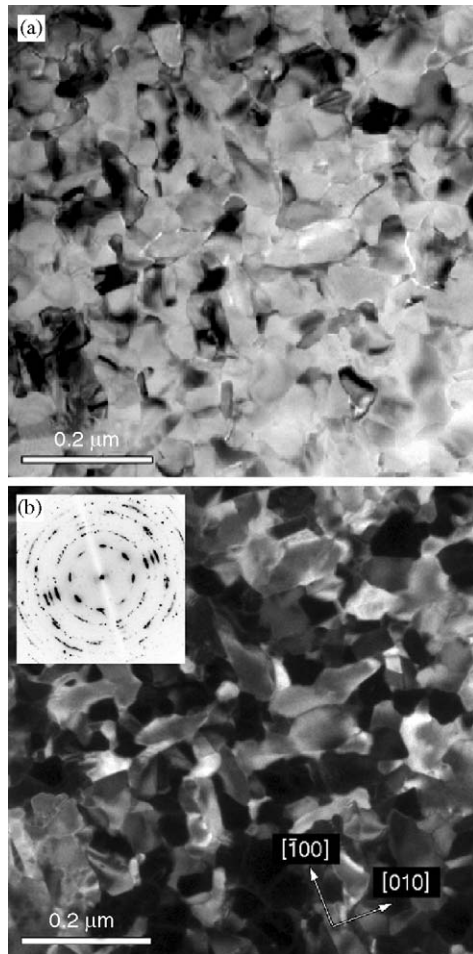


Fig. 1. Bright-field/dark-field image pair of the TiO₂ (anatase) film grown on MgO(001) (beam parallel to MgO[100]). Strong preferred orientation is apparent from the grain shape and alignment. Two anatase orientational variants (at right angles) are present in the diffraction pattern (inset): (a) Bright-field image. (b) Dark-field image of (a) using an anatase 101 reflection (MgO directions are marked).

Diffraction analysis (see later) confirmed that the film was anatase. The rectangular shape of the grains was consistent with the *c*-axis of the tetragonal anatase unit cell being parallel to the (001)MgO surface; this is consistent with the orientation relationship determined (see later). Dark-field imaging using anatase 101 reflections in the diffraction pattern, one of which is shown in Fig. 1b, confirmed the presence of two orientational variants. Different 101 reflections illuminated one of the two sets of

aligned grains. The texturing was more apparent in the dark-field image (Fig. 1b) compared with the bright-field image (Fig. 1a), since the former was formed using a 101 anatase reflection which originated from only one of the two orientational variants, unlike the bright-field image, which shows diffraction contrast from both variants.

Plan-view TEM specimens were made by protecting the coated surface and grinding and ion milling away the substrate. This created a perforation through the film with the region surrounding it comprising only the TiO₂ film. However, further away from this perforation, the MgO substrate was present, and so it was possible to obtain diffraction patterns of only the TiO₂ film, or the TiO₂ and the MgO substrate together. From the latter, it was possible to determine the orientation relationship between the two. Selected-area diffraction from the film with the MgO substrate in place is shown in Fig. 2a. The MgO substrate was viewed along the surface normal, corresponding to MgO[001], and a 4-fold axis of symmetry was evident in the pattern from this phase. Analysis of the measured *d*-spacings from the TiO₂ phase, along with XRD analysis (Fig. 3) confirmed that the film was highly crystalline anatase, with no other phases present. Under identical deposition conditions, anatase was the only phase formed during deposition on Si substrates (oxide-covered or hydride-terminated) [9,10]. Thin TiO₂ films grown on MgO using TiI₄ and either O₂ [12] or H₂O₂ [11] as the precursors (but otherwise very similar conditions to those used here) also found anatase to be the phase formed exclusively at 300 °C. However, at higher temperature some rutile was also formed.

Analysis of the electron diffraction pattern was achieved by calculating the expected pattern (Fig. 2b) on the basis of the proposed orientation relationship. This relationship can be described as

$$\begin{array}{l} \text{MgO} \quad \text{Anatase} \\ [100] \parallel [010] \\ [001] \parallel [100], \end{array} \quad (1)$$

$$\begin{array}{l} [010] \parallel [010] \\ [001] \parallel [100]. \end{array} \quad (2)$$

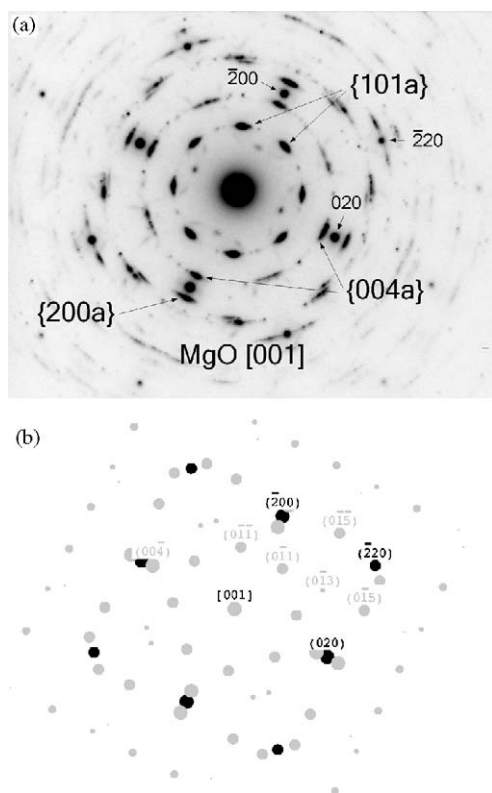


Fig. 2. (a) Selected-area electron diffraction pattern of the anatase film shown in Fig. 1a, viewed along MgO[001]. Both anatase (reflections labelled a) and MgO reflections are present. The orientation relationship proposed (see text) was confirmed by simulating the pattern (b).

The calculated diffraction pattern (Fig. 2b) reproduced all of the major MgO and TiO₂ reflections with the correct orientation. The match was not perfect however, as the film also contained a minor fraction of anatase grains which were randomly oriented. These gave rise to the circular streaking, which the calculated pattern did not recreate (discussed below). The two TiO₂ orientational variants were geometrically equivalent, with a 90° rotation between the two. This relationship is in agreement with similar studies by Schuisky et al. [11,12] who also reported the presence of two variants. The morphology of the anatase grains was consistent with this relationship also. In Fig. 1, the grain morphology reflects the tetrahedral unit cell of anatase. The elongated *c*-axis is parallel to the MgO surface, and the grains occur in two

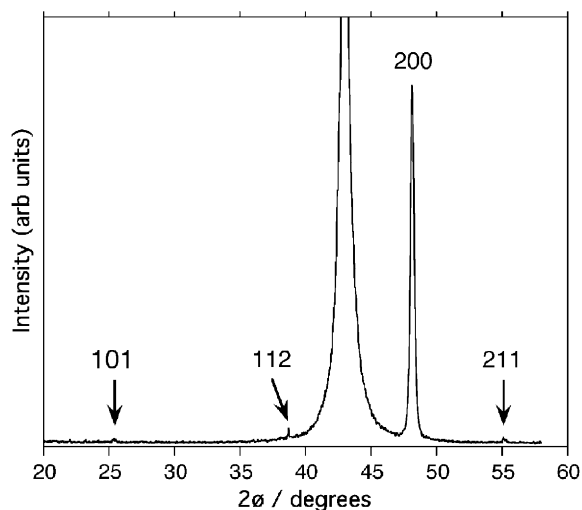


Fig. 3. XRD pattern of TiO₂ on MgO. Indexed peaks are reflections from anatase. The off-scale reflection is due to MgO(001) (substrate).

distinct populations rotated at 90° to each other and aligned with the MgO in-plane cube axes.

Noticeable in the diffraction pattern (Fig. 2a) was the presence of a slight azimuthal smearing in the strongly aligned spots, making them elliptical rather than round. This indicated that there was a small rotation of the aligned grains about a preferred orientation. This is noticeable in the dark-field image (Fig. 1b), in that not all grain boundaries were perfectly aligned parallel to MgO[100] or [010]. Schuisky et al. [11,12] also reported some scatter in crystallite orientation, measured using XRD. The rocking curve full-width at half-maximum measured for the anatase 200 reflection ($\approx 1.5^\circ$ at 300 °C) diminished with increasing deposition temperature, as the films became more strongly textured [11]. In the present work, as well as the aligned anatase reflections, weak diffraction rings were also present, particularly in the higher index reflections. The spacings of these rings are consistent with anatase grains which are randomly oriented. This was evident in the bright-field/dark-field images (Figs. 1a and b) as a number of small equiaxed grains, which do not show the marked tetragonal morphology or faceting of the larger grains. This non-aligned component was also apparent in the XRD pattern

(Fig. 3) where low-intensity anatase reflections were present in addition to the aligned anatase 200 reflection.

To confirm the orientation relationship, electron diffraction patterns were obtained from other low-index MgO zone axes. Figs. 4a and b show an experimental and simulated pattern corresponding to the $[\bar{1}01]$ zone axis of MgO. This orientation of MgO corresponds to the $[1\bar{1}0]$ zone axis of anatase in orientation (1) and is extremely close to the $[502]$ zone axis of anatase in orientation (2). The resulting diffraction pattern (Fig. 4a) is therefore a superposition of the diffraction patterns from $[\bar{1}01]$ MgO, $[1\bar{1}0]$ anatase and $[502]$ anatase. Intense reflections aligned with

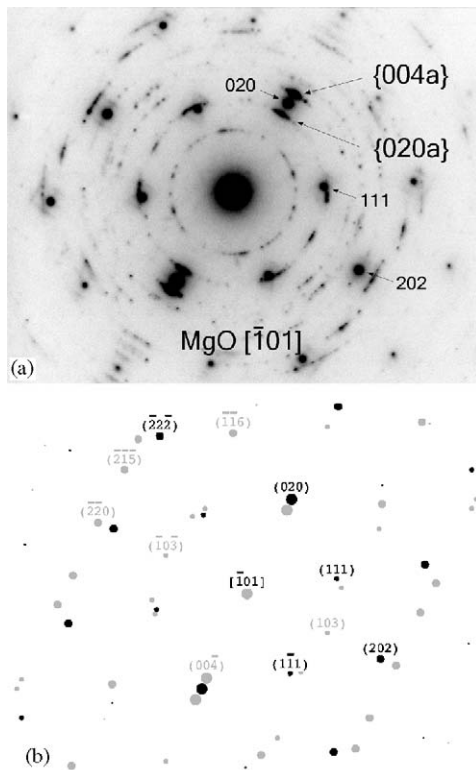


Fig. 4. (a) Selected-area diffraction pattern of the anatase film shown in Fig. 1a, viewed along $\text{MgO}[\bar{1}01]$. This orientation corresponds to $[1\bar{1}0]$ anatase in orientation (1) and is extremely close to $[502]$ anatase in orientation (2). The resulting diffraction pattern is therefore a combination of patterns from these phases/orientations. The simulated pattern (b) reproduces the intensity of the aligned anatase reflections quite well, confirming the previously proposed orientation relationship.

$\text{MgO } 020$ were present. The 004 reflections were due to anatase (orientation 1) and the 020 reflections arose from anatase in orientation (2). The simulated pattern reproduced the pattern due to the aligned anatase well, confirming the proposed orientation relationship.

From the established orientation relationships, it is possible to superimpose real lattice models to understand the likely atomic interactions. Fig. 5 shows the superposition of the anatase $\{100\}$ plane on the $\text{MgO}(001)$ plane with the orientational relationship proposed. There is strong alignment of metal and oxygen atoms between the two phases along the anatase $[001]$ direction, the anatase lattice spacings in this direction being 13.5% greater than the MgO lattice. The lattice mismatch along anatase $[010]$ is somewhat smaller and negative, anatase being -9.6% smaller than the MgO lattice. These lattice mismatches are clearly too great to produce matched epitaxy, but do, nevertheless, provide a strong guiding effect. Similar depositions to these using KBr as a substrate [10], which has the same crystal structure as MgO (cubic), did not result in ordered films. The KBr lattice parameter is 0.6005 nm, compared with just 0.419 nm for MgO. Applying the molecular model approach used here to the KBr situation (not shown) indicates no strong lattice alignments for any of the likely candidate orientations between the two phases.

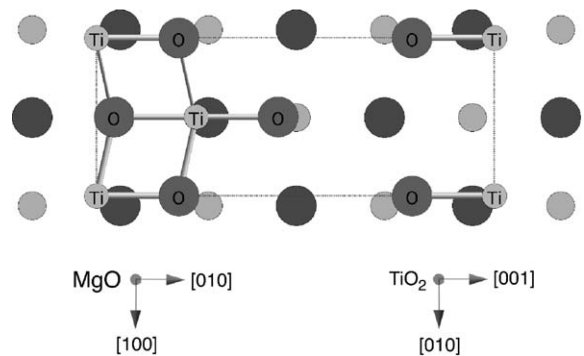


Fig. 5. Schematic representation of the superposition of anatase on MgO using the orientation relationship proposed, showing the atomic alignments which result. Labelled ions are due to anatase. The lower layer (unlabelled) comprises oxygen and magnesium ions.

Our reported growth rate for TiO_2 on silicon substrates, using identical conditions to those used here, was 0.049 nm/cycle [9]. On the MgO substrates, the deposition rate derived from the cross-sectional TEM measurement of film thickness (79 ± 3 nm) was slightly lower at 0.040 nm/cycle. Ellipsometric measurement, which obtains data from a much larger area of the film, gave the film thickness as 86 nm and a corresponding growth rate of 0.043 nm/cycle. Faster growth rates of TiO_2 on MgO, at 0.07 and 0.06 nm/cycle for $\text{TiI}_4\text{-O}_2$ and $\text{TiI}_4\text{-H}_2\text{O}_2$ reaction couples, respectively, have been reported [12], although these rates are for different chemistries to those used here ($\text{TiCl}_4\text{-H}_2\text{O}$) and for a different type of ALD deposition system. While the substrate may exert a strong influence on growth rate during the early stages of deposition, particularly if extended incubation periods for growth are induced, this effect is likely to diminish significantly once the substrate is covered by the growing film.

In order to understand the growth, uniformity and topography of the film, cross-sectional TEM was carried out (Fig. 6). The tendency of the substrate to spontaneously fracture when milled to electron transparency made specimen preparation challenging, since intact film was restricted to regions of the TEM foils which were much thicker than ideal. The grain structure was predominantly columnar; as expected from the geometry of the grains seen in plan-view mode (Figs. 1a and b).

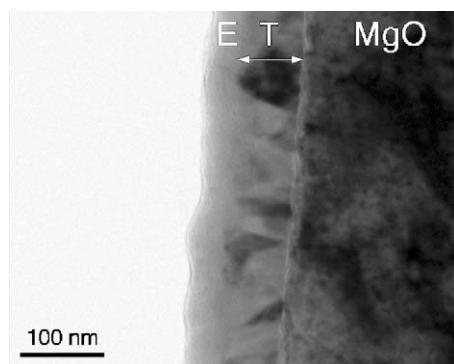


Fig. 6. Cross-sectional TEM image of the anatase (T) film on MgO. The outer surface of the film is coated with epoxy (E) from specimen preparation. The film is 79 ± 3 nm thick, and the grains appear reasonably columnar.

Similar columnar anatase structures have been observed by Schuisy et al. [12]. These columnar grain boundaries correspond to $\{010\}$ planes. The film was highly crystalline and uniform in thickness (79 ± 3 nm). The outer amorphous layer in Fig. 6 is epoxy from TEM specimen preparation. The film outer surface was quite flat, as evidenced by the low standard deviation on the thickness measurements in TEM (± 3 nm) and direct measurement of the roughness average using AFM ($R_a = 6.48$ nm). This is consistent with the proposed orientation relationship, where the upper surface of the film consists of anatase $\{100\}$ planes which are oriented parallel to the substrate. This is in contrast to equivalent films grown on Si substrates, where random orientation results in quite a strong prismatic faceting [9]. This effect produced a flatter surface for films grown on MgO ($R_a = 6.48$ nm) compared with equivalent films grown on Si ($R_a = 10.15$ nm).

4. Conclusions

Deposition of TiO_2 on MgO(100) substrates at 300°C resulted in growth of epitaxial anatase. X-ray and electron diffraction enabled the orientation relationships to be determined. The orientation relationship was consistent with the anatase c -axis lying parallel to the MgO(100) surface in two orientational variants aligned at right angles to each other and being parallel to the in-plane cube axes of the substrate. The morphology of the film reflected this relationship, since the grains were roughly tetragonal with two distinct orientations 90° apart. Elliptical elongation of electron diffraction spots indicated that within the aligned grains, a small degree of rotation about the preferred orientation was present. A small fraction of the film also consisted of randomly oriented anatase grains. Cross-sectional TEM highlighted the general columnar structure, and enabled growth rates to be estimated and compared with those derived from ellipsometric measurement of the film. Cross-sectional TEM and AFM characterisation showed that the films were flatter than equivalent films grown on Si under equivalent conditions. This was consistent with the surface being composed of

grains with (100)anatase planes lying parallel to the substrate, as opposed to the highly prismatic faceting seen in the non-epitaxial anatase.

Acknowledgements

Colleagues in the NanoEngineering team are thanked for their useful discussions. This work was supported by ANSTO.

References

- [1] R.L. Puurunen, *J. Appl. Phys.* 97 (2005) 121301.
- [2] M. Ritala, M. Leskelä, *Nanotechnology* 10 (1999) 19.
- [3] D.R.G. Mitchell, D.J. Attard, K.S. Finnie, G. Triani, C.J. Barbé, C. Depagne, J.R. Bartlett, *Appl. Surf. Sci.* 243 (2005) 265.
- [4] T. Seidel, A. Londergan, J. Winkler, X. Liu, S. Ramnathan, *Solid State Technol.* 43 (2003) 1.
- [5] B. O'Regan, M. Gratzel, *Nature* 353 (1991) 737.
- [6] J. Yu, X. Zhao, Q. Zhao, *Thin Solid Films* 379 (2000) 7.
- [7] A. Rothschild, F. Edelman, Y. Komem, F. Cosandey, *Sensor Actuator B* 67 (2000) 282.
- [8] P. Sawunyama, A. Yasumori, K. Okada, *Mater. Res. Bull.* 33 (1998) 795.
- [9] D.R.G. Mitchell, D.J. Attard, G. Triani, *Thin Solid Films* 441 (2003) 85.
- [10] D.R.G. Mitchell, G. Triani, D.J. Attard, K.S. Finnie, P.J. Evans, C.J. Barbé, J.R. Bartlett, *Device and Process Technologies for MEMS, Microelectronics and Photonics III*, in: J.-C. Chiao, A.J. Hariz, D.N. Jamieson, G. Parish, V.K. Varadan (Eds.), *Proceedings of the SPIE*, vol. 5276, 2004, pp. 296–306.
- [11] M. Schuisky, A. Hårsta, A. Aidla, K. Kukli, A.-A. Kiisler, J. Aarik, *J. Electrochem. Soc.* 147 (2000) 3319.
- [12] M. Schuisky, K. Kukli, J. Aarik, J. Lu, A. Hårsta, *J. Crystal Growth* 235 (2002) 293.
- [13] T. Suntola, *Mater. Sci. Rep.* 4 (1989) 261.